ELSEVIER

Polymer 42 (2001) 8163–8170

polymer

www.elsevier.nl/locate/polymer

Controlled deposition of electrospun poly(ethylene oxide) fibers

J.M. Deitzel*, J.D. Kleinmeyer, J.K. Hirvonen, N.C. Beck Tan

US Army Research Laboratory, Polymers Research Branch Building 4600, AMSRL-WM-MA, APG, MD 21005, USA

Received 2 March 2001; received in revised form 4 May 2001; accepted 7 May 2001

Abstract

Electrospinning is a process by which sub-micron polymer fibers can be produced using an electrostatically driven jet of polymer solution (or polymer melt). Electrospun fibers are typically collected in the form of non-woven mats, which are of interest for a variety of applications including semi-permeable membranes, filters, composite reinforcement, and scaffolding used in tissue engineering. A characteristic feature of the electrospinning process is the onset of a chaotic oscillation of the electrospinning jet. The current work demonstrates the feasibility of dampening this instability and controlling the deposition of sub-micron polymer fibers (<300 nm in diameter) on a substrate through use of an electrostatic lens element and collection target of opposite polarity. Real-time observations of the electrospinning process have been made using high-speed, high-magnification imaging techniques. Fiber mats and yarns electrospun from polyethylene oxide have been analyzed using wide-angle X-ray diffraction (WAXD), optical microscopy, and environmental scanning electron microscopy (ESEM). © 2001 Published by Elsevier Science Ltd.

Keywords: Electrospinning; Nanofibers; Bending instability

1. Introduction

For almost 100 years [1], it has been known that polymer fibers can be generated from an electrostatically driven jet of polymer solution (or polymer melt).

This process, known as electrospinning, has received a great deal of attention in the last decade because of its ability to consistently generate polymer fibers that range from 5 to 500 nm in diameter. Because of the small pore size and high surface area inherent in electrospun textiles [2–4], these fabrics show promise for exploitation in soldier protective clothing and filtration applications [5]. Other applications that are being explored include scaffolding for tissue growth [6], optical and electronic applications [7,8].

The schematic for a typical electrospinning apparatus is depicted in Figs. 1a and 2. The arrows in Fig. 2 denote the direction of the electrostatic field lines and the length the arrows provide a qualitative indication of the field strength (i.e. longer arrows ~ higher field strength). Polymer solution is forced through a syringe needle at a rate of about 0.5 ml/h, resulting in the formation of a drop of polymer solution at the tip of the syringe. A high voltage (5–15 kV) is applied to the syringe needle, causing the surface of the drop to distort into the shape of a cone, as depicted in Fig. 1a. When a critical voltage is exceeded (typically 5 kV for the solutions discussed in this paper), a jet of solution erupts from the apex of the cone and is accelerated toward the electrically grounded collection target by the macroscopic electric field (Fig. 2). As this jet travels through the air, the solvent evaporates leaving behind a polymer fiber to be collected on an electrically grounded target. Fig. 1b is an image of the electrospinning process obtained through high-speed photography. The image clearly depicts the random motion of the electrospinning jet as it travels toward the target. Baumgarten [9] first imaged the chaotic nature of the electrospinning jet motion. Recent work by Reneker et al. [10] suggests that this chaotic motion, or 'bending instability', results (at least in part) from repulsive forces originating from the charged elements within the electrospinning jet. Deposition of electrospun fibers on a stationary target is essentially random due to the chaotic motion of the electrospinning jet as it travels to its target. This is particularly useful for membrane and filter applications, which take advantage of the small pore size obtained by the random morphology of the non-woven electrospun mat.

Collecting electrospun fibers in the form of a yarn or tow for post-processing to improve mechanical performance, or depositing electrospun fibers on a substrate in specific places or patterns is problematic because of the random nature of the fiber deposition. Some efforts to improve the

* Corresponding author. Tel.: +1-410-306-0703.
E-mail address: jdeitzel@arl.army.mil (J.M. Deitzel).

0032-3861/01/$ - see front matter © 2001 Published by Elsevier Science Ltd.
PII: S0032-3861(01)00336-6

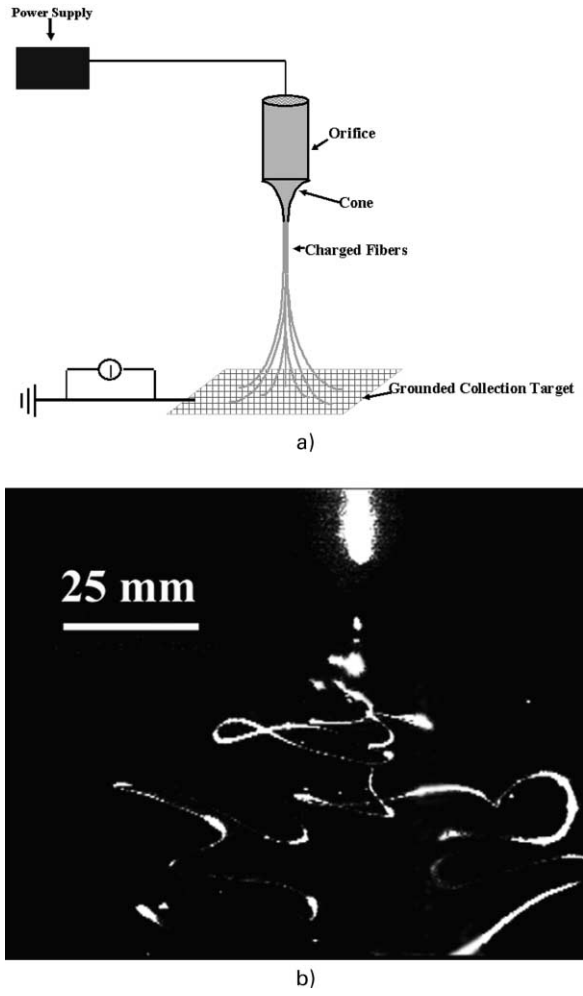

Fig. 1. (a) Standard electrospinning apparatus, (b) High-speed image of electrospinning process.

control over the electrospinning jet and deposition process include the use of both mechanical and electrostatic means. Electrospun fibers can be collected in the form a textile where the fibers will be more or less oriented parallel to the direction of rotation [11] if the target is a drum rotating at high RPMs. However, the area coated with electrospun fibers is still quite large. It has also been shown that electrospun fibers retain a significant portion of their charge upon deposition [2,12], and under the appropriate conditions [12], it is possible to have electrospun fibers deposit preferentially on an aluminum screen forming a three-dimensional grid structure. Finally, Jaeger et al. [13] have demonstrated that it is possible to stop the precession of the electrospinning jet about the tip of the syringe, which contributes to the chaotic motion of the electrospinning jet. This was accomplished by using a single charged ring of like voltage and polarity placed concentrically about the syringe needle. Although this method of electrospinning has the effect of stabilizing the jet at the point of initiation, the jet still undergoes bending instability as it proceeds toward the ground plane after passing through this single electrode region.

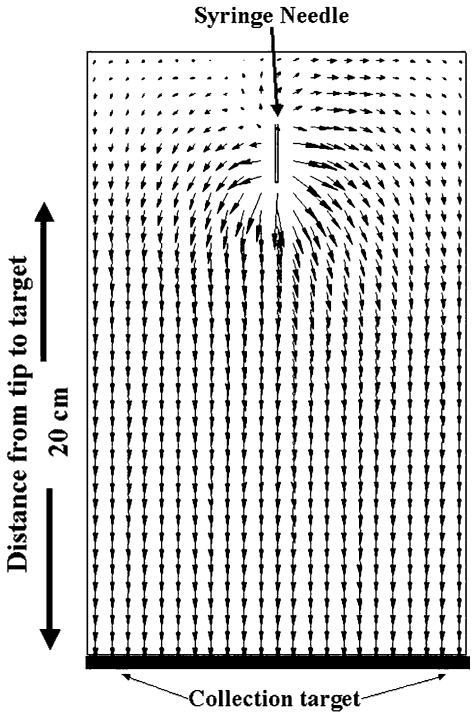

Fig. 2. Field lines calculated for a syringe needle and grounded target geometry.

The objective of the current research has been to construct a novel electrospinning apparatus that uses electrostatic fields, other than the one responsible for jet initiation, to dampen the bending instability inherent in the electrospinning process. It will be shown that this apparatus has allowed for much greater control over the deposition and take-up of electrospun fibers. Wide-angle X-ray diffraction (WAXD) analysis has been performed on electrospun PEO yarns collected using this apparatus, indicating the presence of some molecular orientation and a poorly developed crystalline microstructure within the electrospun fibers.

2. Theory

When an external electric field is applied to a polymer solution, ions in the solution will aggregate around the electrode of opposite polarity. Positive ions travel to the negatively charged electrode and negative ions travel toward the positive electrode. This results in an excess of charge of opposite polarity in the volume of solution near an electrode. Consider a drop of polymer solution suspended at the tip of a metal syringe. When a positive (+) voltage is applied to the metal syringe, the ions in the solution of like-polarity will be forced to aggregate at the surface of the drop. The electric field generated by the surface charge will cause the drop to distort into the shape of a cone [14]. If the electric potential of the surface charge exceeds a critical value [14], the electrostatic forces will overcome

the solution surface tension. A thin jet of solution will erupt from the surface of the cone and travel toward the nearest electrode of opposite polarity, or electrical ground. Although the details of charge motion in the electrospinning jet are not well understood, it is believed that excess charge is essentially static with respect to the moving coordinate system of the jet [10]. This means that the electrospinning jet can be thought of as string of charge elements connected by a viscoelastic medium, with one end fixed at the point of origin and the other end free.

As discussed in Section 1, the free end of the electrospinning jet follows a chaotic path as it travels toward the grounded collection plate, as seen in Fig. 1b. This chaotic motion, or instability, is the result of a complicated interaction of variables that include: viscosity, surface tension, electrostatic forces, air friction, and gravity. Recent work by Reneker et al. [10] has attempted to create a model of jet motion, which takes these variables into account. This effort has met with limited success, although detailed understanding of the jet motion remains elusive. For the present discussion, it is appropriate to focus on the electrostatic forces acting on the charged elements making up the jet and the viscoelastic response of the polymer solution to these electrostatic forces.

In their work, Reneker et al. [10] proposed the following mechanism for the onset of jet instability. Upon initiation, the jet of polymer solution is rapidly accelerated away from the syringe needle toward the grounded target by electrostatic forces. This has the effect of providing a longitudinal stress that stabilizes the jet, keeping it initially straight. At some distance from the point of initiation, the jet of polymer solution starts to undergo stress relaxation. The point along the jet at which this occurs depends on the spinning voltage, which is proportional to the strength of the macroscopic electric field [10]. Increasing the voltage, i.e. the electric field strength increases the length of the stable jet [9]. Once stress relaxation occurs, it was proposed [10] that electrostatic interaction between the charged elements of the jet begins to dominate the ensuing motion, initiating and perpetuating the chaotic motion of the jet. The initiation of the bending instability was described in the following manner.

If one considers three-point unconnected charges of equal value in a line (Fig. 3), it can be seen that the center charge, B, is acted on by two forces of equal magnitude and opposite direction given by the equation,

$$F = kq_a q_b/r^2 = kq_c q_b/r^2 \quad (1)$$

where q_a, q_b and q_c are charges of equal sign and magnitude, r is the separation between charges and k is Coulomb's constant. Should a perturbation cause q_b to move out of line, there is a net lateral force on q_b, the magnitude of which is given by the equation

$$F_l = 2F \cos\theta \quad (2)$$

where θ is the angle that is formed by r and line perpendicular to jet axis. This lateral force, F_l, leads to an inherent

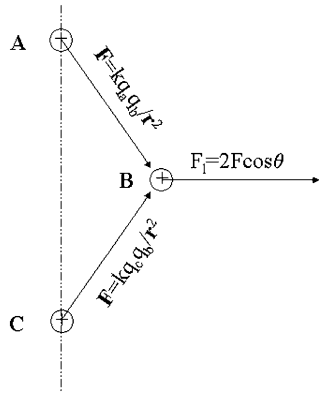

Fig. 3. Forces exerted on a charge element by neighboring charge elements.

instability predicted by Earnshaw's theorem [15]. Since an electrostatically driven jet can be thought of as a line of charged elements, it is thought that the instability predicted by Earnshaw is responsible for the onset of the chaotic motion of the free end of the electrospinning jet [10]. Absent any force to counter F_l, either electrostatic or mechanical in nature, the initially small perturbations grow unfettered leading to the large looping motions that are commonly observed [2,9,10].

The description of the electrospinning process advanced by Reneker et al. suggests that it should be possible to take advantage of basic electrostatic principles to control the electrospinning process. By controlling the shape and strength of the macroscopic electric field between the electrodes (i.e. syringe and collection target), it should be possible to dampen jet instability and to control the deposition of the electrospun fibers on a target. What follows are experimental results demonstrating the feasibility of controlling the electrospinning jet by manipulating the macroscopic electrostatic field in terms of field strength and shape.

3. Experimental

Poly(ethylene oxide) (PEO) fibers were electrospun from a 10 wt% concentration of PEO in water. PEO of 400,000 molecular weight was used in making the solution. Two ES30P power supplies of positive polarity from Gamma High Voltage were used to apply voltages of +5 to +15 kV to the vertically oriented syringe tip and rings. A Glassman Series EH high voltage power supply of negative polarity was used to apply a voltage of −9 to −12 kV to the collection plate situated at the bottom of the apparatus. Polymer solution was fed to the syringe needle tip through a Teflon tube with an 1/8th in. inner diameter using a Harvard 2000 syringe pump. Representations of electric field lines associated with specific electrospinning apparatus were calculated with the computer program, Student's Quick Field™, from Tera Analysis. Electron micrographs of the electrospun fibers were obtained using a Phillips electroscan environmental scanning electron microscope.

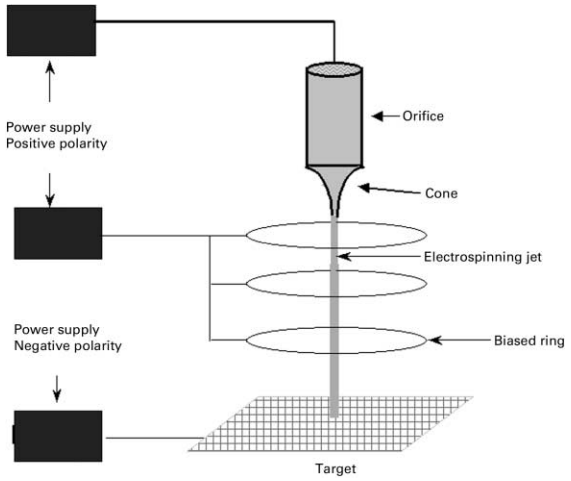

Fig. 4. Multiple field electrospinning apparatus.

High-speed images were taken with a Photometrics cooled CCD camera with a $3K \times 2K$ chip. The camera was attached to a Questar Schmidt–Cassegrain telescope in order to achieve high magnification from a distance of 40 cm. The electrospinning jet was illuminated from behind with a Continuum Surelite II YAG laser. The laser emitted light at a wavelength of 532 nm, having a pulse duration of 10 ns. Optical micrographs of collected fibers were obtained using a Wild Makroscop M420 stereomicroscope.

Yarns of electrospun fibers used in WAXD experiments were collected using a combing technique. This process involved passing two wooden splints spaced approximately 2.0 cm apart repeatedly through the electrospinning jet about 2 cm above the collection target. WAXD analysis was performed using a Rigaku UltraX 18 kW rotating anode X-ray source and a Bruker Hi-Star 2D area detector.

4. Results and discussion

It is clear from the discussion in Section 3 that electrostatic interactions between individual charge elements in the jet and between charge elements and the macroscopic electric field are primarily responsible for initiation and perpetuation of the bending instability. With this knowledge, it should be possible to design an electrospinning apparatus that can dampen or eliminate the bending instability through control of the shape and strength of the macroscopic electric field that exists as a result of the potential difference between the point of jet initiation and the collection target (Figs. 4 and 5). The electrospinning apparatus discussed here is similar to an apparatus first described by Melcher and Warren [16], who were studying capillary instability and jet break-up in electrostatically driven jets of low molecular weight fluids. The apparatus depicted in Fig. 4 is different from the set up illustrated in Figs. 1a and 2 in two ways. The first innovation is a series of charged rings used as an electrostatic 'lens' element that

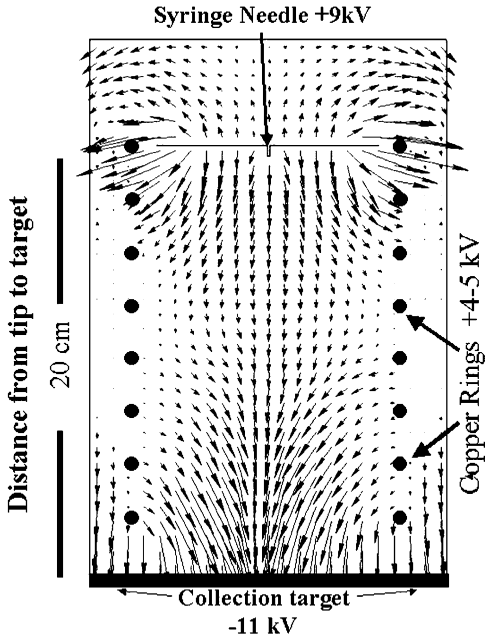

Fig. 5. Field lines calculated for multiple field electrospinning geometry.

changes the shape of the macroscopic electric field from the point of jet initiation to the collection target. The field lines converge to a centerline above the collection target. When the charged jet passes through this field, it is forced to the center in a manner that is analogous to a stream of water that is poured into a funnel. The second difference is that the collection target has a potential bias whose polarity is opposite that of the lens element and syringe needle. This allows for a continuous increase in the electric field strength and a corresponding increase in downward force on the jet as it approaches the collection target (i.e. force $= qE$, where E is the field strength and q the magnitude of the charge element in coulombs).

Fig. 4 is a schematic of the multiple field electrospinning apparatus. The apparatus consists of three high voltage power supplies. The first power supply is positive in polarity and is connected to the syringe needle. This is the source that supplies the critical voltage needed for jet initiation that will be designated as the spinning voltage for the rest of this discussion. The second power supply provides the voltage for eight copper rings that are connected in series. It also provides positive in polarity that will be referred to as the ring voltage. The third power supply is connected to the collection target and it provides negative polarity that will be referred to as the target voltage. The rings are 10 cm in diameter and are spaced approximately at 1.9 cm intervals. The total distance from the tip of the syringe to the collection target is about 20 cm. Values of +9 kV for the spinning voltage, +4 to +5 kV for the ring voltage and −11 kV for the target voltage were usual for a typical experiment.

Fig. 5 is a diagram depicting the macroscopic electric field generated by the apparatus described above. The arrows indicate the direction of the electric field lines. The

electric field is nearly uniform in direction down the center of the apparatus. At the top of the apparatus, there is a tendency for the field lines near the edge of the initiating electrode to point to the rings, which are at a lower potential. About 8 cm from the initiating electrode, the field lines start to converge at the center of the apparatus, indicating a net restoring force that acts on the charge jet. The field strength, and correspondingly the restoring force, increases as the jet approaches the target. On start-up there is some jet instability near the initiating electrode because of the edge effects. As the jet proceeds toward the target, the instability is dampened under the influence the converging electric field lines. Since the jet is continuous, the dampening of the instability and acceleration of the jet downstream act to stabilize the part of the jet near the initiating electrode.

Fig. 6a and b are high-speed images of the electrospinning jet generated with a 7% concentration solution of PEO in water using the apparatus described above. These images were obtained about 10 cm below the syringe tip (half way to the target), which is well into the region where the bending instability normally occurs (see Fig. 1b). Fig. 6a is an image of a straight jet with no evidence of any bending instability. Fig. 6b illustrates the effect of decreasing the ring voltage from +5 to about +2.5 kV. In this case, the jet takes on the shape of a tight corkscrew as a result of relaxing the constraining electric field provided by the rings. When the ring voltage is increased again to 5 kV, the jet straightens out.

Fig. 7a and b shows the images of fiber mats electrospun from a 10% concentration of PEO in water. Fig. 7a was produced using the standard electrospinning method, without biased lens elements. The distance from tip to target was 17 cm and the spinning voltage was about +7 kV at the

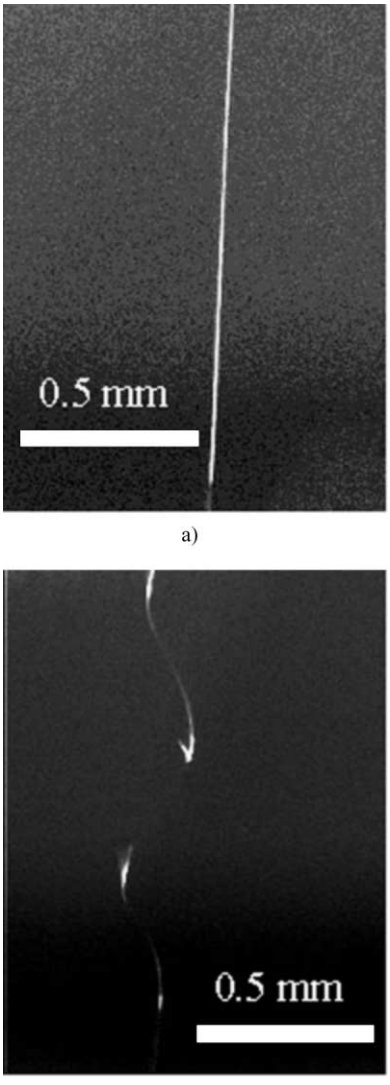

Fig. 6. Image of electrospinning jet 4 in. below capillary orifice: (a) ring electrode potential 2.5 kV; (b) ring electrode potential 5 kV.

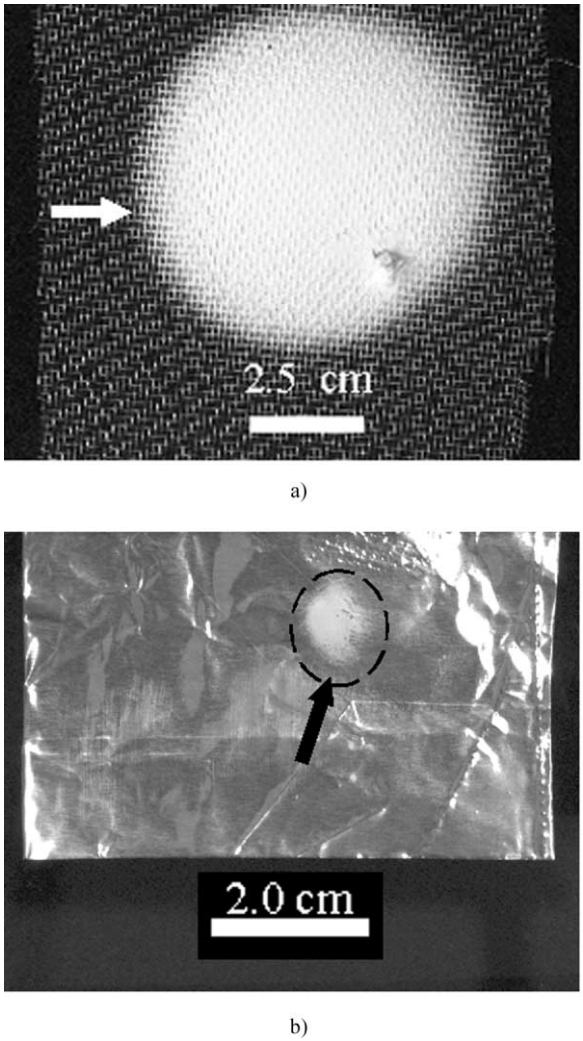

Fig. 7. Arrows indicate area of target covered by electrospun fibers: (a) standard electrospinning technique collected on wire mesh, (diameter ~7 cm); (b) multiple field technique collected on copper foil (diameter ~1 cm). Fibers electrospun from 10% solution concentration of PEO in water.

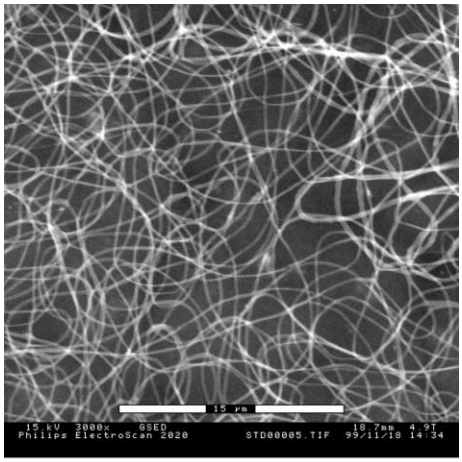

a)

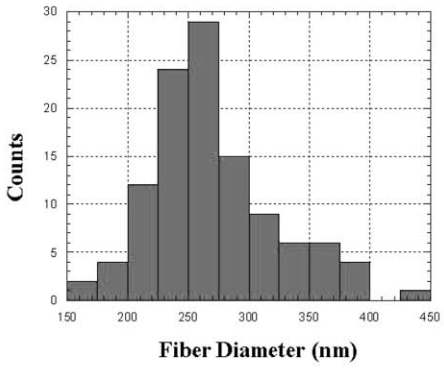

b)

Fig. 8. (a) Electron micrograph of PEO fibers electrospun using multiple field method. (b) Histogram of fiber diameter measurements obtained from (a). Fibers electrospun from 10% solution concentration of PEO in water.

syringe tip and collected on an aluminum screen that was electrically grounded. The fiber mat in Fig. 7b was obtained using the multiple field electrospinning apparatus using positively biased rings orifice and a negatively biased foil collection target. Comparison of these two figures shows the significant decrease in the diameter (from ~7 cm in Fig. 7a to ~1 cm in Fig. 7b) of the area of coverage achieved using the multiple field electrospinning apparatus.

This reduction in the area of coverage is the result of dampening the bending instability. The multiple field technique can also affect the size of the individual fibers. Fig. 8a is an electron micrograph of fibers electrospun from 10% PEO in water using the multiple field technique. The average diameter of the fibers is about 270 nm (Fig. 8b), which compares to an average diameter of 400 nm reported for PEO electrospun from a 10% solution using the standard method of electrospinning, which consisted of a positively biased syringe tip (7 kV), a grounded collection target, and a tip to target distance of about 17 cm^2. It is thought that the reduction in the fiber diameter is due to the fact that overall change in potential from syringe tip to target is much greater for the multiple field apparatus (21 kV) used to collect the

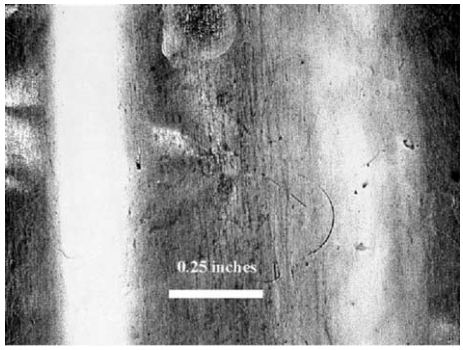

Fig. 9. Electrospun fibers collected on a rotating drum using multiple field electrospinning method.

sample in figure [8,9]. The fibers in Fig. 8 are uniform in their overall morphology and lack beads or junctions, which indicates that most of the solvent has evaporated by the time the fibers are collected on the target.

By dampening the chaotic motion of the jet, it becomes possible to deposit electrospun fibers on a substrate in a more targeted fashion. When the target is a rotating drum covered with copper foil and charged to a potential of −11 kV, the electrospun fibers are collected in a strip that

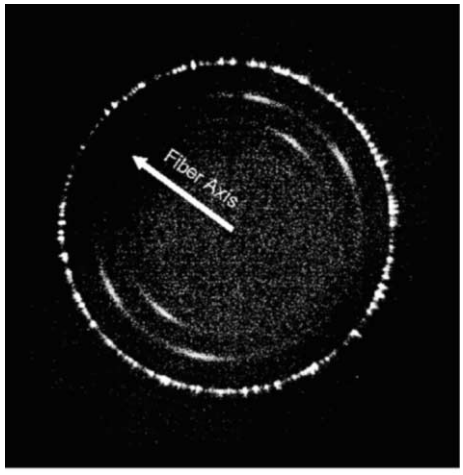

a)

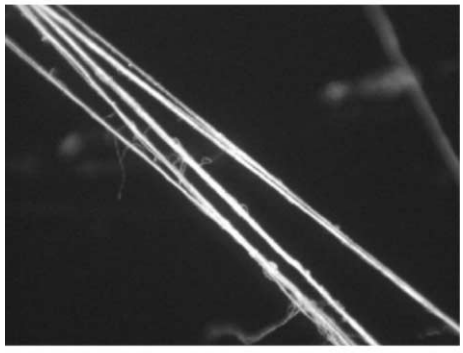

b)

Fig. 10. 2D WAXD pattern (a) obtained from PEO electrospun yarns (b).

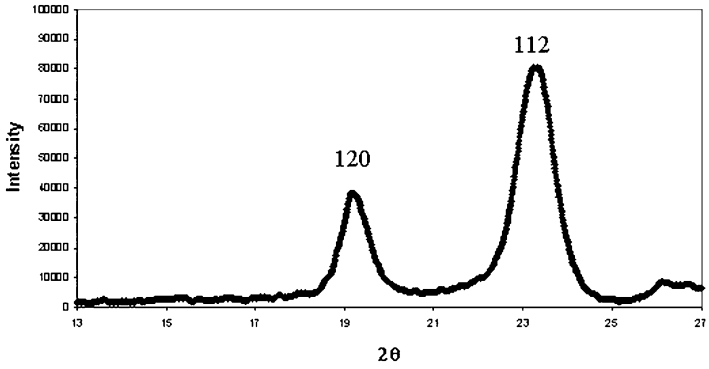

Fig. 11. Plot of the integrated scattering intensity as a function of 2θ from Fig. 10A.

is approximately 0.6 cm wide. Fig. 9 shows two such strips collected within 0.6 cm of each other. Upon start-up, some slight adjustment of the spinning voltage, ring voltage and the solution feed rate are required in order to optimize the control of the deposition process. The strip on the right side of the image was collected during this optimization process and is slightly less well defined. After an hour and a half the drum was shifted slightly to the right and the second well-defined strip was collected under optimized conditions. The collection time for each strip was 1.5 h.

It is also possible to collect electrospun fibers in the form of a yarn with the multiple field apparatus. This was accomplished by a combing technique, where two wooden splints spaced about an inch apart were repeatedly passed between the last ring and the collection plate, through the electrospinning stream. This process allows for the collection of fibers that are more or less macroscopically oriented parallel to the direction of the combing. After 1 h, enough electrospun material was collected for the purpose of WAXD analysis. The fibers were removed from the splints and gently twisted into the yarns seen in Fig. 10b. Fig. 10a is the WAXD pattern obtained for the PEO yarns depicted in Fig. 10b. The pattern shows six diffraction arcs that are characteristic of the monoclinic crystal structure of PEO. The two equatorial reflections correspond to the 120 crystallographic planes and the four arcs in the quadrants correspond to the 112 planes. The particularly intense ring that occurs at $2\theta = 28.44°$ corresponds to the 111 reflection of the silicon powder standard.

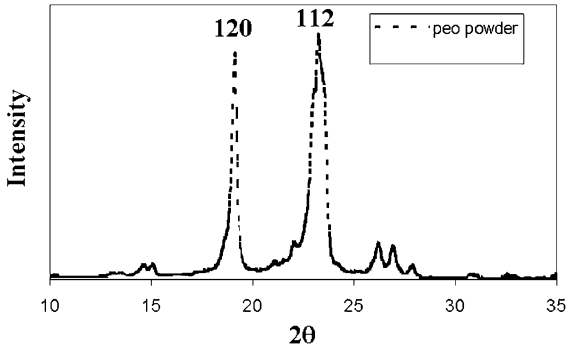

Fig. 12. Powder WAXD pattern for PEO powder.

Fig. 11 is a plot of the integrated intensity of the 2D WAXD pattern in Fig. 10a as a function 2θ. When this figure is compared to a powder WAXD diffraction pattern of PEO (Fig. 12), it can be seen that the 120 and 112 reflections of the fiber pattern are relatively broad and weak with respect to the background. In addition, the powder WAXD pattern of the PEO also contains numerous higher order reflections that are not present in the fiber pattern. The broad, weak nature of the fiber pattern reflections together with the lack of higher order reflections indicates that the crystalline microstructure of the electrospun fibers is not well developed. The fact that the fiber pattern reflections (Fig. 10A) show distinct arcs, rather than isotropic circles like those reported for electrospun polyethylene by Larrondo et al. [17], suggests that some degree of molecular orientation results from this multiple field electrospinning process. It should be noted that no attempts were made to improve the overall crystallinity or the crystal orientation through post process, though it may be possible to improve the degree of order in the multiple field-spun fibers using standard techniques, such as annealing under tension.

5. Conclusion

It has been demonstrated that it is possible to control the deposition of electrospun fibers through the use of an electrostatic lens element and biased collection target. By applying a secondary external field of the same polarity as the surface charge on the jet, it is possible to control or eliminate the bending instability inherent in conventional electrospinning experiments. This mechanism allows for greater control over the deposition of electrospun fiber on a surface and for collection of electrospun fibers in other forms besides non-woven mats. Analyses of yarns of electrospun polyethylene oxide using WAXD techniques indicate the presence of some molecular orientation and a poorly developed crystalline microstructure in the fibers.

Acknowledgements

The authors would like to thank Professor Dan Marble from Tarleten State University for his insightful comments with respect to ion beam optics, and Dr Mike Mcquaide for advice pertaining to high-speed imaging. We would like to thank the American Society of Engineering Education and the Oak Ridge Institute for Science and Education for their support of this work.

References

[1] Zeleny J. Phys Rev 1914;3:69-911078.
[2] Deitzel JM, Kleinmeyer J, Harris D, Beck Tan NC. Polymer 2001;1(42):261–72.
[3] Reneker DH, Chun I. Nanotechnology 1996;7:216–23.
[4] Gibson PW, Shreuder-Gibson HL. US Army Soldier and Biological Chemical Command Technical Report. Natick/TR-99/016L, 1999.
[5] Gibson PW, Shreuder-Gibson HL, Rivin D. AIChE J 1999;45:190–4.
[6] Buchko CJ, Chen LC, Shen Y, Martin DC. Polymer 1999;40:7397–407.
[7] Norris ID, Shaker MM, Ko FK, MacDiarmid AG. Synth Met 2000;114:109–14.
[8] Burgshoef MM, Vancso GJ. Adv Mater 1999;16(11):1362–5.
[9] Baumgarten PK. J Colloid Interf Sci 1971;36:71.
[10] Reneker DH, Yarin AL, Fong H, Koombhongse S. J Appl Phys 2000;87:4531–47.
[11] Doshi J, Reneker DH. J Electrostatics 1995;35:151–60.
[12] Deitzel JM, Beck Tan NC, Kleinmeyer JD, Rehrmann J, Tevault D, Reneker D, Sendijarevic I, McHugh A. Army Research Laboratory Technical Report. ARL-TR-1989, 1999.
[13] Jaeger R, Bergschoof M, Martini I, Batlle C, Schonherr H, Vancso GJ. Macromol Symp 1998;127:141–50.
[14] Tayler GI. Proc R Soc Lond, Ser A 1964;280:383–97.
[15] Jeans J. The mathematical theory of electricity and magnetism. Cambridge: Cambridge University Press, 1958.
[16] Melcher JR, Warren EP. J Fluid Mech 1971;47:127–43.
[17] Larrondo L, John Manley R. J Polym Sci, Polym Phys Ed 1981;19:909–20.